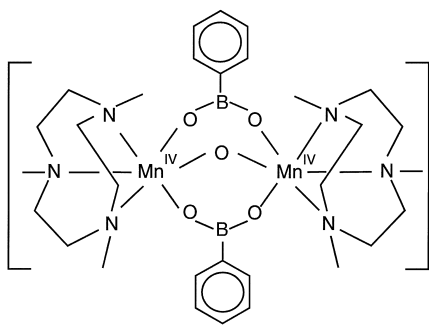


# Integer-Spin Multifrequency EPR Spectroscopy of a Ferromagnetically Coupled, Oxo-Bridged Mn<sup>IV</sup>Mn<sup>IV</sup> Model Complex\*\*

Carole Duboc-Toia,\* Helga Hummel, Eckhard Bill,\* Anne-Laure Barra, Gérard Chouteau, and Karl Wieghardt

Conventional EPR spectroscopy (X-band: 9 GHz (0.3 cm<sup>-1</sup>); Q-band: 35 GHz (1.2 cm<sup>-1</sup>)) has been successfully used to determine the electronic structure of half-integer-spin paramagnets. It has also been applied for the characterization of transition metal ions, with a special focus on metal ion clusters present in biological systems. However, measurements at these frequencies are often insufficient to determine in detail the electronic properties of systems with integer spins or large-spin ground states, especially when the zero field splitting (ZFS) of these systems is larger than or comparable to the microwave quantum. The recent development of high-frequency and high-field EPR (HF-EPR) spectroscopy has allowed the spin Hamiltonian parameters of such compounds to be accurately determined.<sup>[1]</sup>

We illustrate here the use of HF-EPR spectroscopy to study the symmetric, dinuclear, oxo-bridged Mn<sup>IV</sup> complex [L<sub>2</sub>Mn<sup>IV</sup><sub>2</sub>(μ-O)(μ-phBO<sub>2</sub>)<sub>2</sub>](PF<sub>6</sub>)<sub>2</sub> (**1**; L = 1,4,7-trimethyl-1,4,7-triazacyclononane, phBO<sub>2</sub> = phenyl boronic acid).<sup>[2]</sup> This complex is particularly interesting as a model for the high oxidation states observed in several manganese-containing metalloproteins like class IV ribonucleotide reductase<sup>[3]</sup> and the oxygen-evolving complex (OEC) of photosystem II.<sup>[4]</sup> As reported previously,<sup>[2]</sup> the two d<sup>3</sup> Mn<sup>IV</sup> ions are in distorted octahedral N<sub>3</sub>O<sub>3</sub> environments (Scheme 1; av Mn...N 2.117, av Mn...O 1.824 Å). The metal sites with spins S<sub>1</sub> = S<sub>2</sub> = 3/2 are ferromagnetically coupled by an exchange interaction, which leads to a rather unusual ground state for the dimer with a



Scheme 1. Schematic representation of the structure of complex **1**.

[\*] Dr. C. Duboc-Toia, Dr. A.-L. Barra, Prof. G. Chouteau  
Laboratoire des Champs Magnétiques Intenses  
CNRS-MPI

BP 166, 38042 Grenoble Cedex 9 (France)

Fax: (+33)4-76-85-56-10

E-mail: toia@labs.poly.cnrs-gre.fr

Dr. E. Bill, Dr. H. Hummel, Prof. Dr. K. Wieghardt

Max-Planck-Institut für Strahlenchemie

Stiftstrasse 34–36, 45470 Mülheim an der Ruhr (Germany)

Fax: (+49)208-306-3951

E-mail: bill@mpi-muelheim.mpg.de

[\*\*] We thank Dr. S. Gambarelli for the Q-band EPR spectrum.

total spin of  $S=3$ . From a measurement of the magnetic susceptibility of **1** at 1 T as a function of temperature, the coupling constant was determined to be  $J = +10$  cm<sup>-1</sup> ( $H_{\text{ex}} = -2JS_1S_2$ ). The ZFS parameter of Mn<sup>IV</sup> in this analysis was set to zero.<sup>[2]</sup> Variable-temperature variable-field (VTVB) magnetization measurements yield  $|D_1| = |D_2| = 0.7 \pm 0.3$  cm<sup>-1</sup>. The sensitivity of the technique with respect to the local ZFS parameters of the spin-coupled dimer results from the high spin multiplicity of the ground state. This leads to sizable deviations of the magnetization curves at low temperatures from the behavior of a Brillouin function (see Figure 4). The sign of  $D_i$  and the rhombicity parameter  $E/D_i$  could not be determined from the powder data.

Complex **1** exhibits in both frozen acetonitrile solution and in the solid state integer-spin EPR signals at Q-band and X-band frequencies at low temperature (Figure 1). The

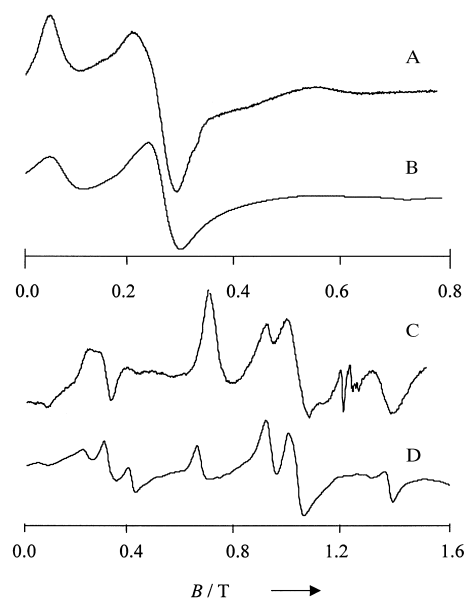


Figure 1. Experimental (A and C) and simulated spectra (B and D) of complex **1** in acetonitrile (0.01 M) recorded at 9.62 (A) and 34.02 GHz (C) at 12 K (parameters are given in the text).

X-band spectra were measured in the perpendicular mode as well as in the parallel mode. The spectra were analyzed by full diagonalization<sup>[5]</sup> of the Hamiltonian for the  $S=3$  spin ground state of the dimer [Eq. (1)]. The effective ZFS of  $S=3$  is represented by the last two terms where  $D_{(S=3)}$  and  $E_{(S=3)}$  gauge the axial and the rhombic parts of the interaction, respectively.

$$H = \beta \mathbf{B} \mathbf{g} \mathbf{S} + D_{(S=3)} [S_z^2 - 1/3S(S+1) + E/D_{(S=3)} (S_x^2 - S_y^2)] \quad (1)$$

Based on the magnetization data the effective  $D$  value can be estimated by spin projection, assuming that the principal axes of the local interactions are colinear.<sup>[6]</sup>  $D_{(S=3)} = 0.2D_1 + 0.2D_2$ . Additionally, the dipolar contributions are neglected in this approach, which is a safe approximation due to the large Mn...Mn separation of 318 pm. For the sake of simplicity, we also did not take into account the contribution of the  $J$  anisotropy. With  $|D_1| = |D_2| \approx 0.7$  cm<sup>-1</sup> a value of

$|D_{(S=3)}| \approx 0.28 \text{ cm}^{-1}$  is obtained. Accordingly, the EPR spectra recorded at 9 and 35 GHz could be simulated reasonably well with effective axial ZFS parameters for the  $S=3$  state in the range  $0.15 < |D_{(S=3)}| < 0.25 \text{ cm}^{-1}$ .

With increasing temperatures up to 150 K no low-frequency EPR signals could be observed from excited states of the coupled spin system. This is unexpected since the  $S=2$  state is only about  $60 \text{ cm}^{-1}$  above the ground state ( $\Delta E = 6 \text{ J}$ ), and the spin projection coefficient for the conversion of the intrinsic ZFS is equal to zero for the quintet. Therefore, a derivative spectrum should be observed around  $g=2$ . We assume that fast spin relaxation, including transitions between the spin multiplets, sets on as soon as excited multiplets are thermally populated and thus broadens the  $S=2$  spectra.

Furthermore, the X- and Q-band spectra of the ground state are very broad and difficult to simulate in the usual spin-Hamiltonian approach, even if distributions of  $D$  and  $E/D$  are included to account for possible sample inhomogeneities. It might be that weak intermolecular spin couplings in the solid and in the concentrated solutions cause severe distortions of the spectra. Therefore, HF-EPR spectroscopy is essential to accurately analyze the zero-field parameters and the  $g$  tensor of this ferromagnetically coupled  $\text{Mn}^{\text{IV}}$  model compound with an  $S=3$  spin ground state.

The HF-EPR experiments were performed on polycrystalline powder samples of complex **1**. The spectra were recorded at two different frequencies (190 and 285 GHz) in the temperature range of 5 to 145 K on a home-built spectrometer.<sup>[7]</sup> The complete spectra obtained at 285 GHz and with measurement at 10 and 103 K are shown in Figure 2.<sup>[8]</sup> With

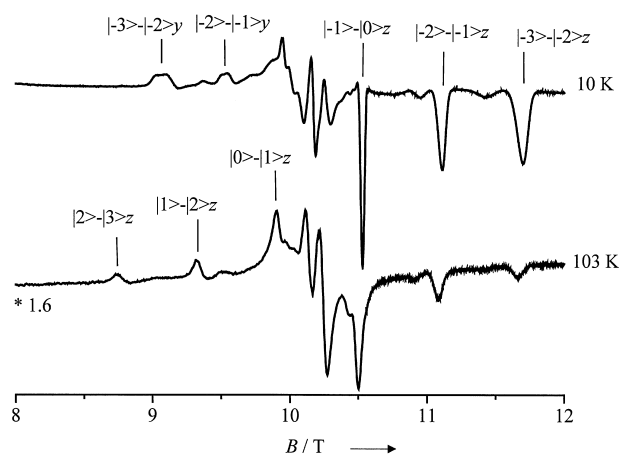


Figure 2. High-frequency EPR spectra (285 GHz) of polycrystalline complex **1** at 10 K (top) and 103 K (bottom). Particular EPR transitions of the  $S=3$  multiplet for  $B_0$  along the molecular  $z$  and  $y$  directions are labeled with the  $|M_s\rangle$  quantum numbers of the respective ground and excited states and the magnetic orientation ( $z$ :  $B_0$  along  $z$ ;  $y$ :  $B_0$  along  $y$ ). The spectrum recorded at 103 K is depicted with an amplification factor of 1.6 for clarity.

increasing temperature, three effects due to Boltzmann statistics are observed as expected: 1) The overall intensity of the spectrum decreases. 2) The relative intensities of the EPR transitions between different Zeeman levels ( $M_s$ ,  $M_{s+1}$ ) of the  $S=3$  multiplet change. For instance, at 10 K the transition at 11.7 T is stronger than that at 11.1 T; the opposite

behavior is seen at 103 K. 3) Higher  $M_s$  levels are populated and, hence, additional transitions are observed.

An important feature of low-temperature HF-EPR spectra is that they directly provide the sign of the ZFS parameter  $D$ . This results from the fact that the strong fields of HF-EPR induce Zeeman splittings larger than  $kT$  at 4.2 K, which leads to significant differences in the populations of the  $M_s$  levels. Under this condition, if  $D < 0$ , the transitions along the  $z$  axis are expected to occur at the low-field side of the resonances centered around  $g \approx 2$ , while the reverse is true for  $D > 0$ .<sup>[1e]</sup> Here the features associated with the  $z$  component of the  $S=3$  multiplet are observed at high field at low temperature, which shows us that  $D_{(S=3)}$  is positive. The assignment of the six derivative signals related to the expected  $g_z$  transitions, as indicated in Figure 2, was achieved from the temperature dependence of the spectra. At low temperature  $y$  transitions between the  $-3 \rightarrow -2$  and  $-2 \rightarrow -1$  levels are also observed at 9.1 and 9.5 T. Qualitative assignments for other transitions are not possible due to the fact that many spectral contributions corresponding to the different orientations overlap.

A first estimate of the  $D$  value can be obtained directly from the experimental spectrum recorded at 10 K. At high field limits the difference between the resonance fields of two subsequent  $z$  transitions is  $2D/g_z\beta$ . The corresponding resonances for the  $M_s = -3, -2$ , and  $-1$  levels of **1** are observed at 11.7, 11.1, and 10.5 T, respectively (Figure 2). This yields a field difference of 0.6 T, corresponding to a  $D_{(S=3)}$  value of about  $0.28 \text{ cm}^{-1}$ .

The HF-EPR spectra of **1** were simulated by using a full-matrix diagonalization procedure for the spin Hamiltonian [Eq. (1)].<sup>[9]</sup> Since in this case the calculated transitions are very sensitive to all the parameters ( $D$ ,  $E$ , and  $g$ ) due to the relative strengths of the zero-field and Zeeman interactions at high field, the values and signs of the ZFS parameters  $D_{(S=3)}$  and  $E_{(S=3)}$  could be accurately determined, and the different components of the  $g$  tensor were obtained. The best simulated spectrum at 50 K is shown in Figure 3. The intensity, the

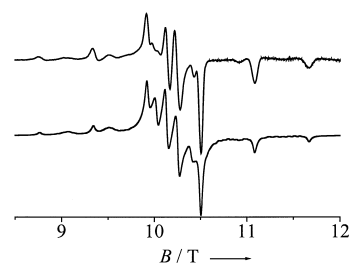


Figure 3. Experimental (top) and simulated powder HF-EPR spectrum (bottom) of polycrystalline complex **1** at 285 GHz and 50 K (parameters are given in the text).

position, and the shape of the simulated spectrum are in good agreement with the experimental data. The spin Hamiltonian parameters used for this simulation are  $D_{(S=3)} = 0.27 \pm 0.01 \text{ cm}^{-1}$ ,  $E_{(S=3)} = 0.05 \pm 0.01 \text{ cm}^{-1}$ ,  $g_{x(S=3)} = 1.990 \pm 0.001$ ,  $g_{y(S=3)} = 1.993 \pm 0.001$ , and  $g_{z(S=3)} = 1.994 \pm 0.001$ . The magnitude of the rhombicity parameter  $E/D_{(S=3)} = 0.185$  and of the corresponding single ion values reflect the asymmetric quasi-octahedral environment of the  $\text{Mn}^{\text{IV}}$  ion with three short Mn–O and three longer Mn–N bond lengths.

Biomimetic models of metalloenzymes may be helpful in determining the structure of the metal ion site and in elucidating the biological role of the metal cluster. It is also essential to study the models in solution. In an attempt to determine the electronic structure of **1** in solution, EPR measurements were performed at 285 GHz in acetonitrile (0.01M) at 5 K. The experimental data were simulated successfully with the same set of parameters determined above for the solid as well as with the low-frequency EPR data in acetonitrile (Figure 1). However, in solution the resolution is relatively poor due to broadening of the signals. We assume that this is caused by microinhomogeneities in the frozen matrix. The fact that the (average) ZFS parameters are the same in solution and in the solid state reveals identical coordination geometries of the manganese ions in the two states.

The magnetization data of solid **1** could be reevaluated<sup>[10]</sup> by using the exact ZFS parameters from the HF-EPR data, which were converted into values for single ions:  $D_1 = D_2 = 0.68 \text{ cm}^{-1}$  ( $0.2 D_1 + 0.2 D_2 = D_{(S=3)}$ ),  $E_1/D_1 = 0.19$  ( $= E/D_{(S=3)}$ ). An excellent simulation of the experimental VTVB magnetization data and temperature dependence of the molar magnetic susceptibility was achieved with  $J = +11.4 \text{ cm}^{-1}$  (Figure 4), if in addition to the explicit ZFS an intermolecular coupling was introduced by means of a mean-field approximation with a Weiss constant of  $\Theta = 0.27 \text{ cm}^{-1}$ . The effect of this coupling was not observed in the high-field spectra, presumably due to the strong fields which decouple the molecules.

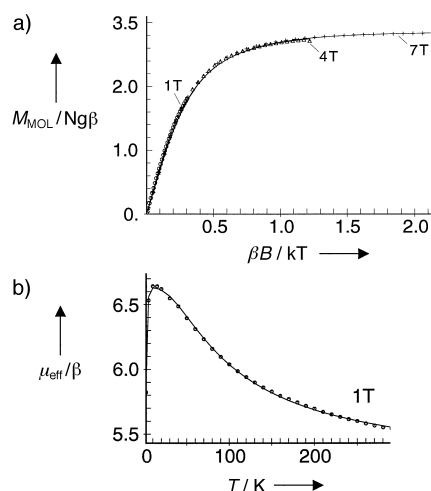


Figure 4. Static magnetization data of polycrystalline complex **1**. The solid lines are derived from a simulation based on a spin Hamiltonian description of exchange interaction, single-ion zero-field and Zeeman interactions (parameters are given in the text). a)  $M_{\text{MOL}}$  = magnetization per mole,  $B$  = applied magnetic field. b)  $\mu_{\text{eff}}$  = effective magnetic moment.

Temperature- and frequency-dependent EPR investigations combined with VTBT magnetization measurements have been successfully applied to characterize the electronic structure of a spin-coupled system. The spin-Hamiltonian parameters of the  $S=3$  ground state have been fully determined by simulation of the patterns obtained by HF-EPR on powders and frozen solutions. The ZFS is positive with a moderate value for  $D_{(S=3)}$  and an unexpectedly high

value for  $E_{(S=3)}$  ( $E/D_{(S=3)} = 0.185$ ), which could not be deciphered from the low-frequency EPR studies. Considering the number of metal ion clusters that are present in enzymatic systems, but which have still not been fully characterized due to a lack of effective methods, the use of new spectroscopic techniques in biology is required. The ability to obtain high-quality spectra in solution makes the use of HF-EPR even more attractive, especially for proteins containing clusters whose characterization by classic EPR is insufficient or ineffective.

Received: February 25, 2000

Revised: May 17, 2000 [Z14761]

- [1] a) A.-L. Barra, D. Gatteschi, R. Sessoli, G. L. Abbati, A. Cornia, A. C. Fabretti, M. G. Uytterhoeven, *Angew. Chem.* **1997**, 109, 2423; *Angew. Chem. Int. Ed. Engl.* **1997**, 37, 2329; b) D. P. Goldberg, J. Telser, J. Krzystek, A. G. Montalban, L.-C. Brunel, A. G. M. Barrett, B. M. Hoffman, *J. Am. Chem. Soc.* **1997**, 119, 8722; c) J. Telser, L. A. Pardi, J. Krzystek, L.-C. Brunel, *Inorg. Chem.* **1998**, 37, 5769; d) M. J. Knapp, J. Krzystek, L.-C. Brunel, D. H. Hendrickson, *Inorg. Chem.* **1999**, 38, 3321; e) A.-L. Barra, L.-C. Brunel, D. Gatteschi, L. A. Pardi, R. Sessoli, *Acc. Chem. Res.* **1998**, 31, 460; f) S. M. J. Aubin, N. B. Maple, L. Pardi, J. Krzystek, M. W. Wemple, L.-C. Brunel, M. B. Maple, G. Christou, D. N. Hendrickson, *J. Am. Chem. Soc.* **1998**, 120, 4991; g) A.-L. Barra, A. Caneschi, A. Cornia, F. Fabrizi de Biani, D. Gatteschi, C. Sangregorio, R. Sessoli, L. Sorace, *J. Am. Chem. Soc.* **1999**, 121, 5302.
- [2] U. Bossek, H. Hummel, T. Weyhermüller, K. Wieghardt, S. Russell, L. van der Wolf, U. Kolb *Angew. Chem.* **1996**, 108, 1653; *Angew. Chem. Int. Ed. Engl.* **1996**, 35, 1552–1554.
- [3] A. Willing, H. Follman, G. Auring, *Eur. J. Biochem.* **1988**, 170, 603.
- [4] V. K. Yachandra, V. J. DeRose, M. J. Latimer, I. Mukerji, K. Sauer, M. P. Klein, *Science* **1993**, 260, 675.
- [5] C. Krebs, E. Bill, H. Hummel, modified version of IRON-HS and SPEGIRON (B. J. Gaffney, J. Silverstone in *Biological Magnetic Resonance*, Vol. 13 (Eds.: L. J. Berliner, J. Reuben), Plenum, New York, **1993**, unpublished).
- [6] A. Bencini, D. Gatteschi, *Electron Paramagnetic Resonance of Exchange Coupled Systems*, Springer, Berlin, **1990**.
- [7] a) A.-L. Barra, L.-C. Brunel, J. B. Robert, *Chem. Phys. Lett.* **1990**, 165, 107; b) F. Muller, M. A. Hopkins, N. Coron, M. Grynberg, L.-C. Brunel, G. Martinez, *Rev. Sci. Instrum.* **1989**, 60, 3681.
- [8] At 190 GHz and 10 K (data not shown) features are present between 5.4 and 8.8 T, demonstrating that the spectrum at 10 K shown in Figure 2 is complete.
- [9] C. J. H. Jacobsen, E. Pedersen, J. Villardsen, H. Weihe, *Inorg. Chem.* **1993**, 32, 1216.
- [10] C. Krebs, E. Bill, F. Birkelbach, V. Staemmler, JULIUS, simulation program for magnetization data using full matrix diagonalisation routines, unpublished.